13th International Conference on
Structural Health Monitoring of Intelligent Infrastructure
DOI: 10.3217/978-3-99161-057-1-046

Structural Health Monitoring of a suspended steel infrastructure: A statistical approach

Nicola Molon[1], Filippo Casarin[2], Alessandro Targa[3], Renzo Codato[4], Francesca da Porto[1]

[1] University of Padova, Dept. of Geosciences, Via Gradenigo 6, 35131 Padova, Italy
[2] Expin srl, via Pisacane 34, 35138 Padova, Italy
[3]Alessandro Targa – studio di ingegneria, viale dell'Industria 23/B – 35129 Padova, Italy
[4] Veneta Sanitaria Finanza di Progetto S.p.a., via Paccagnella 11, 30174 Mestre, 30174 - Venezia, Italy

email: nicola.molon@phd.unipd.it, casarin@labexpin.com, alessandro@studiotarga.com, rcodato@vsfp.it, francesca.daporto@unipd.it

ABSTRACT: The inspection, maintenance and monitoring of existing infrastructure are critical aspects for ensuring a proper structural performance during their lifespan, also guaranteeing their capacity vs. the ultimate limit state. The use of structural health monitoring systems has become increasingly important for managing infrastructural assets, not only to detect structural damages and degradation phenomena but also to evaluate the performance of structures subjected to retrofit interventions. This is achieved using signal processing techniques that integrate statistical methods and machine learning algorithms within the framework of statistical pattern recognition. The proposed framework introduces a novel statistical analysis framework aimed at characterizing the *normal* behaviour of structures, detecting potential damage development. The method is applied to a suspended steel truss healthcare facility, demonstrating its effectiveness in characterizing its typical structural behaviour, detecting any onset of possible structural decay. While the method is demonstrated on a specific case study, it is designed to be adaptable to a wide range of structural systems. The ultimate objective is to develop a reliable analysis tool for the early detection of damage, thereby enhancing the efficiency of maintenance strategies and ensuring long-term structural safety.

KEY WORDS: Structural health monitoring, statistical pattern recognition, damage detection, data analysis.

1 INTRODUCTION

Infrastructure systems play a crucial role in modern society, making it essential to ensure their functionality under both normal and extraordinary loading conditions. Maintenance, inspections, and structural monitoring are fundamental for preserving resilience [1]. In recent decades, traditional inspection systems have been increasingly replaced by structural health monitoring (SHM) systems, particularly for structures that are highly exposed to atmospheric actions and external loads, such as bridges and wind turbines [2], but also for historical buildings [3], [4]. SHM has been introduced to support owners and authorities to find optimal life-cycle management solutions and, ultimately, to prevent structural failures. This is achieved through a damage identification strategy, which encompasses the detection, diagnosis, and prognosis of damage [5].

These systems rely on the implementation of a monitoring-based strategy, which includes real-time measurement of structural responses and data analysis to identify anomalies and/or damage at an early stage [6]. In this context, damage is defined as any alteration in the material and/or geometric properties of bridge components that negatively affect the bridge's current or future service performance and safety [5]. Another significant application of SHM systems involves the assessment of retrofit interventions on existing structures. Specifically, SHM can be used to determine the most suitable intervention strategy, evaluate the structural response after the intervention, and monitor the structure's behaviour throughout the different phases of the intervention [7], [8].

This study proposes a robust framework for processing SHM data from existing infrastructure, with the goal of enabling early detection of structural anomalies or damage. The proposed methodology combines time series modelling using statistical algorithms for the characterization of normal structural behaviour, filtering out environmental influences—such as temperature—and identifying deviations indicative of potential structural issues.

The manuscript is structured as follows: Section 2 describes the case study and presents the initial analyses conducted on the structure; Section 3 introduces the SHM data and provides preliminary evaluations; Section 4 details the proposed data analysis framework and its application to the case study; finally, Section 5 presents the conclusions and outlines directions for future research.

2 DESCRIPTION OF THE CASE STUDY

The analysed structure is a suspended steel truss that serves as the roof of a strategic infrastructure located in northern Italy. The building was completed in 2008. This structure is particularly complex because, as illustrated in Figure 1, the truss system supports the upper three floors through steel columns subjected to tensile stresses. The roof is directly connected to continuous concrete walls that extend from the foundations to the roof.

The building, and specifically its roof, underwent a retrofit intervention aimed at enhancing the strength of the connections within the roof structure. Following the retrofit process, the installation of a SHM system was defined with the objective of assessing the effectiveness of the strengthening interventions, monitoring the real time safety conditions of the structure, and supporting infrastructure owners in identifying optimal life-cycle management solutions.

DOI: 10.3217/978-3-99161-057-1-046

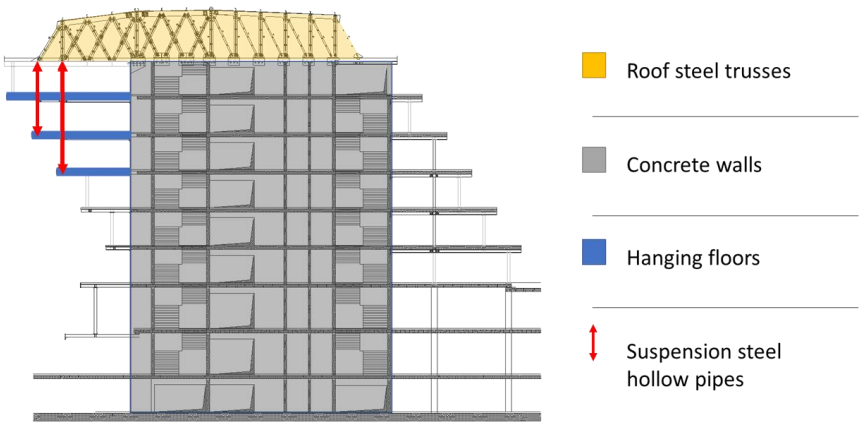

Figure 1. Schematic representation of the structure

2.1 Operational modal analysis of the case study

Before the design of the SHM system an operational modal analysis (OMA) was performed with the aim of identify dynamic parameters of the steel truss structure and better understand the complex behaviour of the entire steel structure. This type of analysis is commonly performed on various types of structures like bridges [9], historical buildings [10], and timber structures [11].

The OMA was performed by installing eight piezoelectric monoaxial accelerometers in different positions and configurations on the roof, resulting in a total of 33 measurement locations. The results of the modal identification are presented in Figure 2.

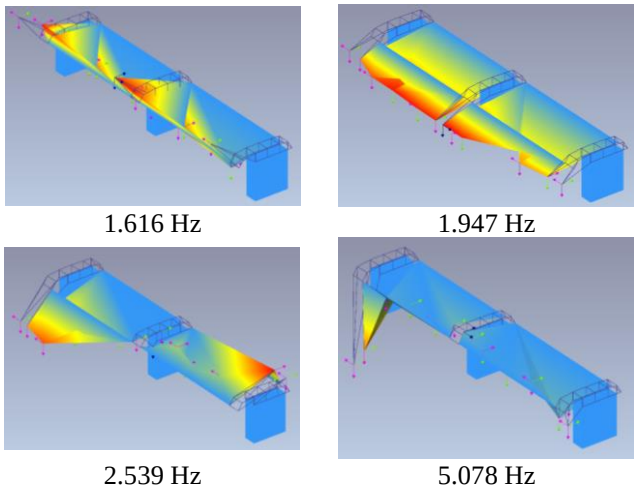

Figure 2. First mode shapes of the structure

These results indicate that the longitudinal and transverse modes exhibit a behaviour involving the overall structure, whereas vertical modes are related to individual truss elements, without demonstrating a global structural response.

Table 1 presents the modal frequencies and the corresponding complexity of the mode shapes obtained from the OMA analysis. The analysis was conducted using the frequency domain decomposition method with Artemis Modal Pro software.

Table 1. Principal vibration frequencies

Mode type	Frequency [Hz]	Complexity [%]
1st Longitudinal	1.66	0.899
1st Transversal	1,953	1,741
2nd Transversal	2,539	5,886
1st Vertical	5,078	18,075
2nd Vertical	16.992	6.052
3rd Vertical	17.969	19.657

2.2 Description of the monitoring system

The SHM system was installed in 2021 to monitor both static and dynamic parameters, enabling the acquisition of the structure's modal characteristics and the evaluation of stress in the most heavily loaded elements of the truss roof. Additionally, thermocouples and ambient temperature sensors were implemented to assess the environmental conditions of the site, as temperature is one of the primary sources of variability in structural systems [12]. The setup for the analysis of vibration characteristics was based on the results of the OMA analysis reported in section 2.1. In this context, 11 uniaxial piezoelectric accelerometers were installed on the steel truss elements.

Ambient temperature sensors were installed in two different locations to assess variations in ambient temperature and humidity within the roof structure. Additionally, a wind sensor was used to investigate potential interactions between this external load and the structural behaviour of the building.

The data acquisition system selected for the monitoring system is structured around a primary acquisition unit (master), which is connected to the infrastructure's LAN for remote data transmission. This master unit is linked to two subordinate units (slaves) via a backbone running along the extrados of the roof, which, in turn, are connected to both static and dynamic sensors. Figure 3 shows the configuration of the SHM system implemented for the case study.

The evaluation of stresses was conducted through the installation of 24 vibrating wire strain gauges on the truss elements, equipped with an internal temperature sensor, complemented by 4 steel thermocouples to assess the influence of temperature on the steel elements. Both types of sensors were welded onto the steel elements of the roof structure, as shown in the configuration presented in Figure 4. A relevant

DOI: 10.3217/978-3-99161-057-1-046

number of sensors was installed on the vertical steel elements connecting the lower floors to the roof, as these components are critical to the floor stability.

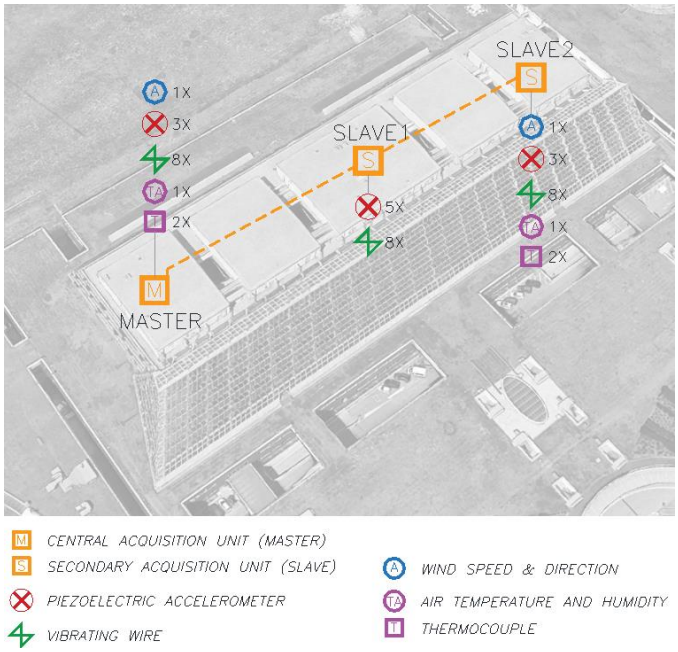

Figure 3. Configuration of the SHM system

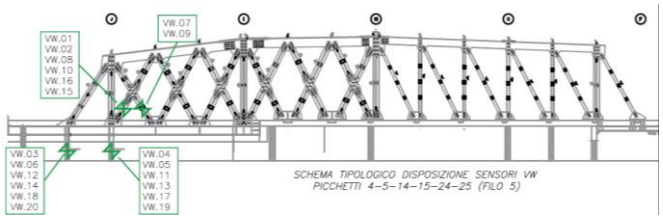

Figure 4. Typological configuration of vibrating wire strain gauges and thermocouple sensors in the truss structure

3 ANALYSIS OF THE MONITORED DATA

In this paper, only the data related to the static sensors are presented, with a particular focus on the analysis of strain sensor measurements.

Figure 5 illustrates the strain behaviour over a three-year period for five sensors. In some of that, such as VW.01 and VW.03, strain variations closely follow seasonal temperature fluctuations. Conversely, in other cases, such as VW.02, the strain behaviour appears independent of temperature variations.

This observation is further emphasized by analysing the correlation between strain sensor data and temperature variations. In Figure 6 the strain measurements are plotted against ambient temperature fluctuations to assess the extent to which thermal effects influence structural behaviour. This comparative analysis helps distinguish temperature-dependent responses from other potential factors affecting strain variations.

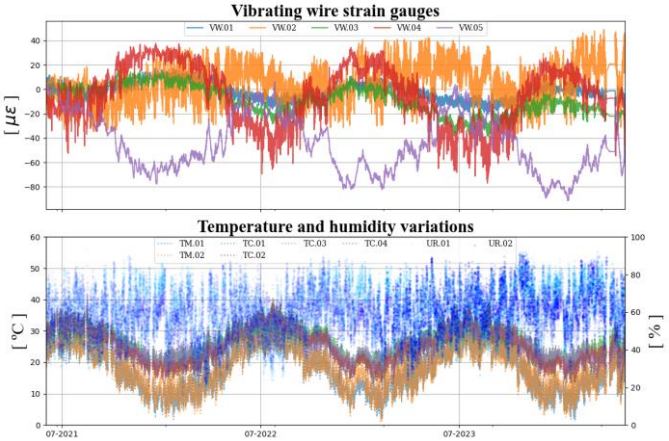

Figure 5. Strain sensors behaviour – block A

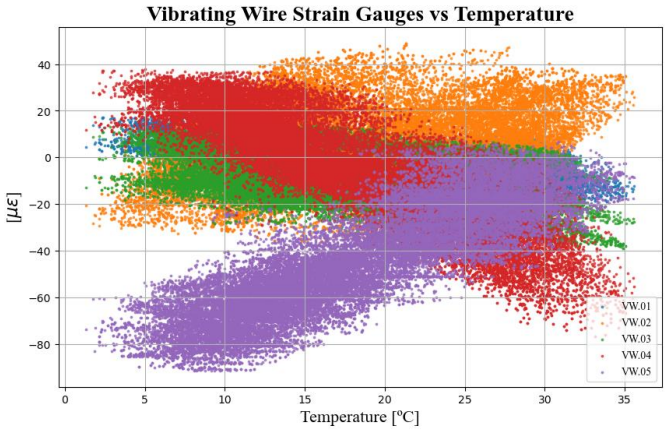

Figure 6. Representation of the strain observation against the temperature value

The behaviour of some sensors exhibits a linear correlation with temperature, whereas others do not show this dependence, as observed in the cases of VW.02 and VW.06. Noticeably, VW.02 appears to be completely uncorrelated with temperature; however, distinct patterns can still be identified. Specifically, its behaviour reflects a horizontal translation of an inclined line along the horizontal axis.

This pattern is influenced by temperature variations occurring during specific periods of the year. When analysing the behaviour of an individual sensor in relation to temperature, with measurements categorized by month (Figure 7), it becomes evident that each period of the year corresponds to a distinct structural state of the element. Furthermore, after one year, the sensor's behaviour tends to return to a state similar to that of the previous year, indicating a recurring annual trend.

After an on-site inspection, it was found that this behaviour was likely caused by friction grip bolted connections which, due to possible loss of preload, converted into standard shear connections. As a result, the structural elements exhibited a different behaviour compared to the expected response of roof elements subjected to daily and seasonal temperature variations. It emerged that some sensors exhibited a typical linear relationship with temperature variations, while others displayed a distinct behaviour characterized by multiple linear trends that were temperature dependent.

DOI: 10.3217/978-3-99161-057-1-046

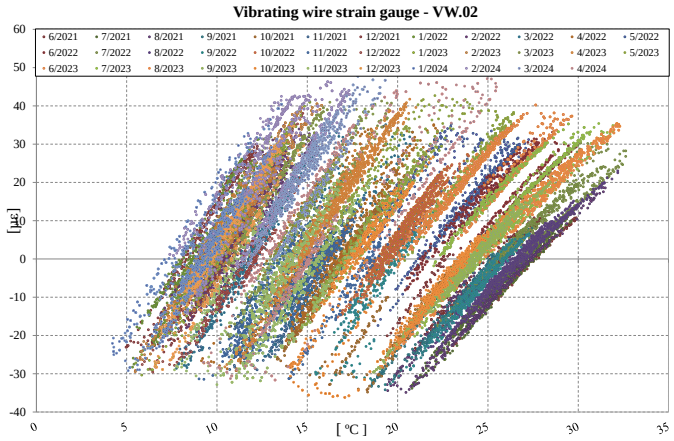

Figure 7. Representation of strain sensor respect to external temperature, divided by period

4 STATISTICAL ANALYSIS OF THE STATIC SENSORS

The adopted methodology consists of several phases. First, a data-cleaning process is performed on the raw data and the entire timeseries was divided in three different groups: train dataset, covering two years, in which the statistical algorithm was trained; validation dataset, spanning in the next ten months, used to define the warning and the alarm boundaries for the control chart; and the test dataset consisting on thirty days, using to validate the entire statistical process. In this phase also an under sampling was performed and the median of each four hours was assumed like the values.

Then, for each sensor, a time series model is estimated to capture the natural variations in the data while accounting for daily and seasonal cycles. By employing this approach, the estimated model effectively represents the expected sensor behaviour under normal operating conditions. Additionally, the model enables the removal of the influence of steel temperature, from the signal.

The developed monitoring system is designed to track real-time prediction errors generated by each estimated model. Specifically, a control chart is implemented for each sensor, based on a statistical control metric and equipped with alert and alarm thresholds. The control chart triggers an alarm when deviations from the expected behaviour are detected. Furthermore, it is designed to differentiate between temporary anomalies and structural anomalies, as specified in the system requirements.

4.1 Statistical model development

The forecasting methodology used in this study is based on the seasonal autoregressive integrated moving average with exogenous variables (SARIMAX) model. This class of autoregressive models is extensively applied in SHM to detect structural anomalies, particularly in time series data analysis for damage identification [5], [13]. By leveraging past observations and incorporating external influencing factors, SARIMAX models effectively characterize the expected behaviour of a system over time [14].

In this application, temperature readings from thermocouples served as exogenous inputs. The autoregressive (AR) components define the present response as a function of previous observations, while the moving average (MA) components refine predictions by accounting for past errors. To enhance accuracy, the model also integrates seasonal components to capture periodic fluctuations occurring on both daily and annual scales. The generalized formulation of this model is expressed as:

$$\begin{aligned}(1-B)^d(1-B)^D y_t &= \phi_1 y_{t-1} + \phi_2 y_{t-2} + \cdots + \phi_p y_{t-p} \\ &+ \Phi_1 y_{t-s} + \Phi_2 y_{t-2s} + \cdots \\ &+ \Phi_P y_{t-Ps} + \theta_1 \epsilon_{t-1} + \theta_2 \epsilon_{t-2} \\ &+ \cdots \theta_q \epsilon_{t-q} + \Theta_1 \epsilon_{t-s} + \Theta_2 \epsilon_{t-2s} \\ &+ \cdots \Theta_Q \epsilon_{t-Qs} + \epsilon_t + \beta X_t\end{aligned} \quad (1)$$

Where:

- B is the lag operator, such that:

$$\begin{aligned}(1-B)y_t &= y_t - y_{t-1} \\ (1-B^s)y_t &= y_t - y_{t-s}\end{aligned} \quad (2)$$

- $\phi_1, \ldots, \phi_p$ are the autoregressive parameters.
- $\theta_1, \ldots, \theta_q$ are the moving average parameters.
- $\Phi_1, \ldots, \Phi_P$ are the seasonal autoregressive parameters.
- $\Theta_1, \ldots, \Theta_Q$ are the seasonal moving average parameters.
- ϵ represents an error term, assumed to follow a Gaussian distribution.
- X_t represents the temperature recorded by the temperature.

The selection of the model, including the determination of the parameters p, d, q, P, D, Q, as well as the subsequent estimation of model coefficients, was guided by the second-order Akaike information criterion. This criterion was employed to optimize model selection by balancing goodness-of-fit and complexity, ensuring an optimal trade-off between model accuracy and overfitting.

The results of the models for the sensor VW.01 are presented in Figure 8 were the entire time series was reported, and in Figure 9 were only the results for the test dataset is presented. The figures show the relatively low and uncorrelated behaviour of the residuals that's denotes the good behaviour of the algorithm for this type of analysis.

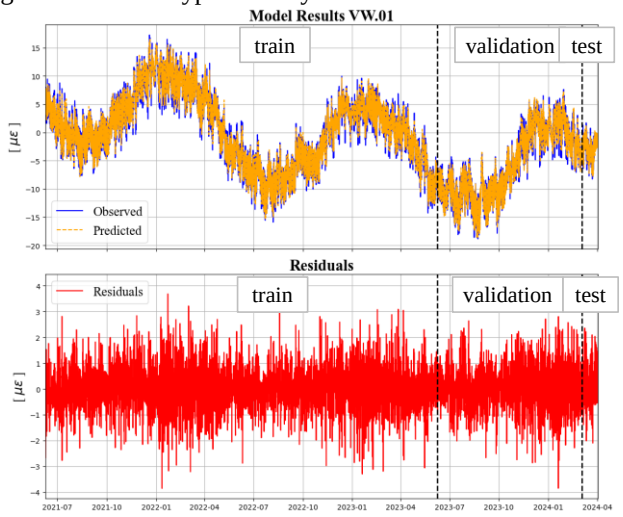

Figure 8. Representation of the results of the SARIMAX model for the entire time series for sensor VW.01

DOI: 10.3217/978-3-99161-057-1-046

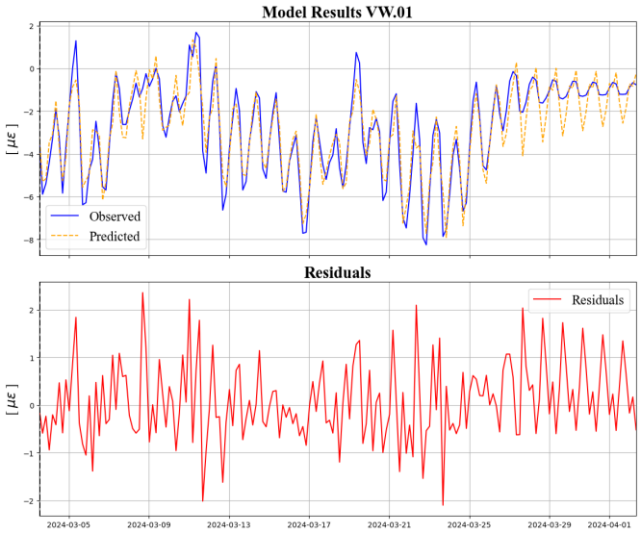

Figure 9. Representation of the SARIMAX model for the test dataset for sensor VW.01

In Table 2, different metrics are presented to compare the model's performance for the analysed sensors. The used metrics include root mean square error (RMSE), mean absolute error (MAE), median absolute error (MedAE), and the coefficient of determination (R^2) for the test dataset residuals.

The model's performance demonstrates generally strong predictive capability, with high R^2 values in most cases. A subset of three sensors exhibits optimal performance, characterized by minimal error metrics and an R^2 of 0.99, indicating an excellent model fit. Another group of ten sensors shows good performance, with moderate error values yet maintaining high R^2, suggesting the model effectively captures underlying patterns. However, five sensors present higher error values, with some displaying lower R^2, particularly those with RMSE exceeding 2, which may indicate limitations in the model's predictive accuracy for these cases.

Table 2. Residuals metrics values

Sensor	RMSE	MAE	MedAE	R2
VW.01	0.81	0.63	0.52	0.86
VW.02	0.94	0.69	0.55	0.99
VW.03	0.93	0.71	0.56	0.92
VW.04	1.35	0.98	0.73	0.94
VW.05	0.62	0.42	0.25	0.99
VW.06	0.60	0.38	0.25	0.99
VW.07	1.08	0.85	0.70	0.99
VW.08	1.17	0.83	0.61	0.99
VW.09	2.26	1.74	1.36	0.97
VW.10	2.68	1.95	1.41	0.77
VW.11	0.37	0.29	0.23	0.99
VW.12	1.08	0.78	0.51	0.95
VW.13	2.64	1.90	1.47	0.88
VW.14	2.02	1.48	1.08	0.93
VW.15	1.53	1.20	1.01	0.99
VW.16	1.03	0.75	0.61	0.99
VW.17	1.31	0.97	0.68	0.88
VW.18	1.25	0.95	0.74	0.80
VW.19	1.77	1.30	0.81	0.96
VW.20	0.69	0.52	0.40	0.99

4.2 *Control chart development*

For the monitoring phase, an adaptive exponentially weighted moving average (AEWMA) control chart is proposed [15], [16]. This type of control chart integrates exponential smoothing with an adaptive mechanism that allows for a faster response to significant changes. As a result, the control statistic is dynamic and adjusts based on observed variations.

The mathematical formulation of this adaptive statistic is given by:

$$S_i = S_{i-1} + \varphi(x_i - S_{i-1}) \tag{3}$$

Where φ is defined as:

$$\varphi(e) = \begin{cases} e + (1-\lambda)k & se\ e < -k \\ \lambda e & se\ -k \le e \le k \\ e - (1-\lambda)k & se\ e > k \end{cases} \tag{4}$$

The advantage of this generalization lies in its ability to enable the control statistic to respond more rapidly to abrupt and high-intensity deviations, specifically when $|e| > k$. In this case the values used for the analysis are $\lambda = 0.1$ e $k = 3$ [15].

By incorporating exponential smoothing, the AEWMA control chart is able to detect anomalies that develop gradually over time. However, its adaptive nature also allows for the identification of sudden, unexpected deviations.

This adaptability will later be leveraged to distinguish transient anomalies, which return to a normalized operational state within a short time frame. In essence, this type of control chart enables differentiation between structural anomalies, which persist over time, and transient anomalies, which resolve naturally after a brief period.

4.3 *Definition of warning and alert boundaries*

To determine the warning and alarm thresholds associated with the control statistic described in the equation (3), a statistical approach is employed based on the concept of mean time to false alarm. Specifically, the average run length (ARL_0) represents the expected number of observations that occur before a false alarm is triggered.

The selection of alert thresholds is carried out by specifying a predefined ARL_0 value. Once this value is established, the corresponding threshold can be determined using statistical simulation techniques.

In particular, the thresholds are computed to ensure compliance with the ARL_0 criterion through the bisection method, as discussed in Qiu (2013) [17]. This approach ensures that the alarm system maintains a controlled balance between sensitivity and reliability.

4.4 *Results of the analysis*

In this section the results for the application of the AEWMA control chart for different sensors are shown. Figure 10 reports the results of the AEWMA control chart and the boundaries definition for the test dataset of the sensor VW.01. It shows a good behaviour that has value around zero, even if in the last part the behaviour of the control chart denotes a linear trend that is contained into the defined boundaries elsewhere.

DOI: 10.3217/978-3-99161-057-1-046

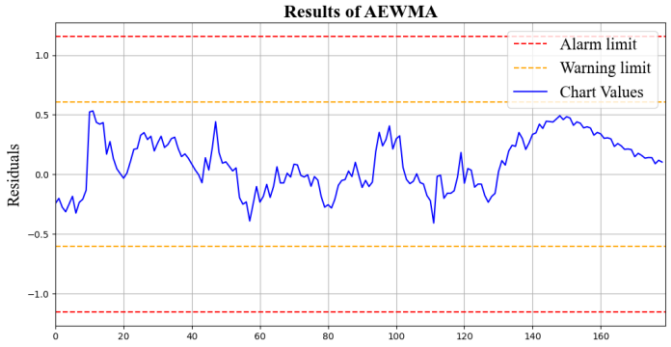

Figure 10. Control chart for VW.01 test dataset

In Table 3 the boundaries for all the vibrating wire sensors are reported. It shows that the value of the boundaries is different one to each other and, clearly, the higher value is related to the timeseries that shows more difficulties for the model to fit the data and determine higher residuals value also in Table 2. But, caused by the limits were defined with the same ARL_0, we aspect that the resilience of the control chart is the same for all the sensors.

Table 3. Evaluation of the boundaries of each sensor

Sensor	RMSE	MAE	MedAE	R2
VW.01	0.607	1.156	0.607	1.156
VW.02	3.735	8.950	3.735	8.950
VW.03	1.258	2.729	1.258	2.729
VW.04	8.620	10.540	8.620	10.540
VW.05	0.878	6.292	0.878	6.292
VW.06	0.318	1.150	0.318	1.150
VW.07	4.264	5.465	4.264	5.465
VW.08	15.821	35.360	15.821	35.360
VW.09	5.335	7.336	5.335	7.336
VW.10	7.513	20.983	7.513	20.983
VW.11	0.372	0.542	0.372	0.542
VW.12	1.624	3.294	1.624	3.294
VW.13	11.633	16.041	11.633	16.041
VW.14	7.964	9.995	7.964	9.995
VW.15	6.237	8.872	6.237	8.872
VW.16	5.176	9.579	5.176	9.579
VW.17	3.223	7.446	3.223	7.446
VW.18	21.752	37.891	21.752	37.891
VW.19	7.421	10.413	7.421	10.413
VW.20	3.031	6.434	3.031	6.434

4.5 Manual introduction of external perturbations

This paragraph analyses the behaviour of the control chart when different outliers appear in the time series.

In this case, an outlier was manually introduced into the test measurements. The variation was added at observation number 50 in the test dataset, with a value equal to twice the standard deviation of the validation dataset (12.0με). The control chart (Figure 11) shows two consecutive outliers at the point where the anomaly was introduced, indicating an isolated change in sensor behaviour.

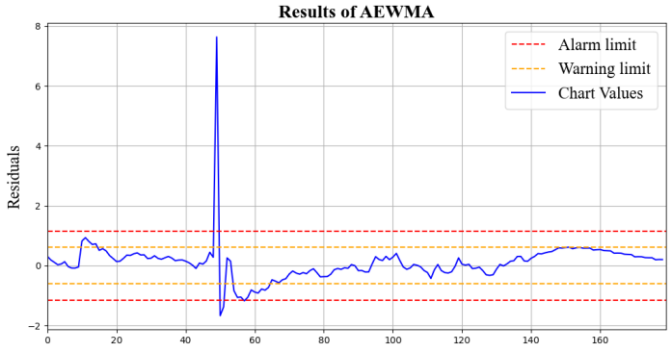

Figure 11. Control chart found with introduction of instant changing of the timeseries

Instead, if a constant shift or a linear trend occurs at the same point in the time series, the variation in the control chart differs from the previous case. In Figure 12 a constant shift equal to twice the standard deviation of the validation dataset was introduced. Notably, in the subsequent observation of the time series, there is no opposite variation in the values.

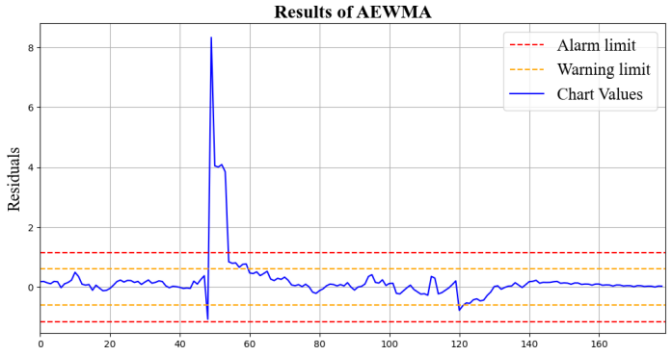

Figure 12. Control chart found with introduction of shift in the observations

This analysis demonstrates how different types of anomalies can be detected using this statistical approach and how variations in the control chart can help distinguish between them. Specifically, it allows for the differentiation between instantaneous sensor variations and constant offsets or linear trends in the time series. These distinctions can differentiate appropriate maintenance strategies for both the structure and the SHM system itself.

Moreover, this type of control, associated with the first data cleaning phase, makes it possible to differentiate issues related to data acquisition—such as corrupted signals—which may result in uncorrelated spikes within the time series. These anomalies can be separated from other types of perturbations, such as constant shifts, linear trends, and correlated spikes, which are more likely to be associated with structural phenomena.

5 CONCLUSIONS

This article proposes a statistical approach for continuously evaluating data collected from SHM systems, supporting infrastructure authorities in making informed decisions for the life-cycle assessment of their assets. The proposed framework individually analyses static sensors along with their associated

DOI: 10.3217/978-3-99161-057-1-046

external variables—in this case, thermocouples—to define the system's normal behaviour.

A SARIMAX model is applied to identify both long-term and short-term patterns in the sensor measurements, assess correlations with external variables, and filter out their effects from the data. Subsequently, the residuals are monitored using an AEWMA control chart, which does not only consider the current residual value but also accounts for deviations from previous residuals. This method further enables the differentiation of various types of anomalies.

The control chart within the proposed framework enables the differentiation of various types of signal perturbations associated with different forms of structural degradation. Additionally, the data cleaning process and the control chart allow for the distinction between these structural anomalies and those arising from data acquisition issues.

For this case study, the framework demonstrated effective performance. The next phase of this research involves extending the framework to groups of sensors, ensuring that potential sensor-specific issues do not trigger unnecessary alarms or warnings for infrastructure authorities, thereby improving the robustness of the monitoring system. In the future, it will also be necessary to apply this type of control to various types of structures to verify and confirm its effectiveness under different conditions and with varying input parameters. This will help assess the system's reliability and adaptability across various structural and environmental scenarios.

ACKNOWLEDGMENTS

Part of the work presented in this paper includes outcomes derived from a research contract between ADEL srl and the Department of Statistical Sciences at the University of Padova.

REFERENCES

[1] M. Pina, L. Mehmet, and Ç. Editors, “Seismic Structural Health Monitoring From Theory to Successful Applications.” [Online]. Available: http://www.springer.com/series/15088

[2] E. Figueiredo and E. Cross, “Linear approaches to modelling nonlinearities in long-term monitoring of bridges,” *J Civ Struct Health Monit*, vol. 3, no. 3, pp. 187–194, Aug. 2013, doi: 10.1007/s13349-013-0038-3.

[3] F. Lorenzoni, F. Casarin, M. Caldon, K. Islami, and C. Modena, “Uncertainty quantification in structural health monitoring: applications on cultural heritage buildings,” 2014.

[4] F. Lorenzoni, F. Casarin, C. Modena, M. Caldon, K. Islami, and F. da Porto, “Structural health monitoring of the Roman Arena of Verona, Italy,” *J Civ Struct Health Monit*, vol. 3, no. 4, pp. 227–246, Dec. 2013, doi: 10.1007/s13349-013-0065-0.

[5] E. Figueiredo and J. Brownjohn, “Three decades of statistical pattern recognition paradigm for SHM of bridge,” 2022. [Online]. Available: http://hdl.handle.net/10871/129482

[6] C. R. Farrar and K. Worden, “An introduction to structural health monitoring,” *Philosophical Transactions of the Royal Society A: Mathematical, Physical and Engineering Sciences*, vol. 365, no. 1851, pp. 303–315, Feb. 2007, doi: 10.1098/rsta.2006.1928.

[7] A. Pierdicca, F. Clementi, P. Mezzapelle, A. Fortunati, and S. Lenci, “One-year monitoring of a reinforced concrete school building: Evolution of dynamic behaviour during retrofitting works,” in *Procedia Engineering*, Elsevier Ltd, 2017, pp. 2238–2243. doi: 10.1016/j.proeng.2017.09.206.

[8] S. Fan, L. Ren, H. Li, and B. Song, “Real-Time Monitoring and Early Warning Method Utilizing FBG Sensors in the Retrofitting Process of Structures,” *Int J Distrib Sens Netw*, vol. 2015, 2015, doi: 10.1155/2015/359549.

[9] A. Gennaro, A. Caprino, V. Pernechele, F. Lorenzoni, and F. da Porto, “In-situ test and model updating of an RC tied-arch bridge,” in *Procedia Structural Integrity*, Elsevier B.V., 2022, pp. 822–829. doi: 10.1016/j.prostr.2023.01.107.

[10] F. Casarin, N. Molon, and D. Talozzi, “OMA and dynamic SHM of the Urbino Cathedral struck by the 2016 central Italy seismic events,” in *Proceedings of the 10th International Operational Modal Analysis Conference (IOMAC 2024)*, IOMAC 2024, 2024.

[11] M. Salvalaggio, F. Lorenzoni, and M. R. Valluzzi, “Impact of sound-insulated joints in the dynamic behaviour of Cross-Laminated Timber structures,” *Journal of Building Engineering*, vol. 91, Aug. 2024, doi: 10.1016/j.jobe.2024.109525.

[12] H. Sohn, “Effects of environmental and operational variability on structural health monitoring,” *Philosophical Transactions of the Royal Society A: Mathematical, Physical and Engineering Sciences*, vol. 365, no. 1851, pp. 539–560, Feb. 2007, doi: 10.1098/rsta.2006.1935.

[13] H. Sohn, C. R. Farrar, N. F. Hunter, and K. Worden, “Structural health monitoring using statistical pattern recognition techniques,” *Journal of Dynamic Systems, Measurement and Control, Transactions of the ASME*, vol. 123, no. 4, pp. 706–711, 2001, doi: 10.1115/1.1410933.

[14] Charles. R. Farrar and K. Worden, *Structural health monitoring: a machine learning perspective*. Wiley, 2013.

[15] G. Capizzi and G. Masarotto, “An Adaptive Exponentially Weighted Moving Average Control Chart,” 2003.

[16] A. Mitra, K. B. Lee, and S. Chakraborti, “An adaptive exponentially weighted moving average-type control chart to monitor the process mean,” *Eur J Oper Res*, vol. 279, no. 3, pp. 902–911, Dec. 2019, doi: 10.1016/j.ejor.2019.07.002.

[17] Qiu Pehiua, “Introduction to Statistical Process Control,” 2013. Accessed: Mar. 05, 2025. [Online]. Available: https://doi.org/10.1201/b15016